

Full Self-Consistent Projection Operator Approach to Nonlocal Excitations in Solids

Yoshiro KAKEHASHI^{1*}, Tetsuro NAKAMURA¹, and Peter FULDE^{2,3}

¹*Department of Physics and Earth Sciences, Faculty of Science, University of the Ryukyus,
1 Senbaru, Nishihara, Okinawa, 903-0213, Japan*

²*Max-Planck-Institut für Physik komplexer Systeme, Nöthnitzer Str. 38, D-01187 Dresden, Germany*

³*Asia Pacific Center for Theoretical Physics, Pohang, Gyeongbuk 790-784, Korea*

A self-consistent projection operator method for single-particle excitations is developed. It describes the nonlocal correlations on the basis of a projection technique to the retarded Green function and the off-diagonal effective medium. The theory takes into account long-range intersite correlations making use of an incremental cluster expansion in the medium. A generalized self-consistent coherent potential is derived. It yields the momentum-dependent excitation spectra with high resolution. Numerical studies for the Hubbard model on a simple cubic lattice at half filling show that the theory is applicable in a wide range of Coulomb interaction strength. In particular, it is found that the long-range antiferromagnetic correlations in the strong interaction regime cause shadow bands in the low-energy region and sub-peaks of the Mott-Hubbard bands.

KEYWORDS: non-local excitations, momentum-dependent self-energy, Hubbard model, ARPES

1. Introduction

Single-particle excitations play an important role in condensed matter physics. They determine among others basic properties of solids such as the metal-insulator (MI) transition, magnetism, and superconductivity.¹ Recently developed angle-resolved photoemission spectroscopy allows to observe details of the excitation spectra in various materials.^{2,3} The excitations are usually strongly influenced by electron correlations. Therefore various approaches to treat the correlations have been developed. Hubbard,^{4,5} for example, was the first who proposed a theory of the MI transition on the basis of the retarded Green function. He derived lower and upper Mott-Hubbard incoherent bands caused by strong electron correlations. Cyrot⁶ extended the theory to finite temperatures by using the functional integral method. Penn⁷ and Liebsch⁸ developed a Green function theory starting from the low-density limit using the t-matrix approximation. Fulde *et al.*⁹⁻¹³ proposed methods which use the projection technique. The latter describes the dynamics of electrons by means of the Liouville operator on the basis of the retarded Green functions.

*E-mail address: yok@sci.u-ryukyu.ac.jp

In the past two decades single-site theories of excitations with use of an effective medium have extensively been developed. Progress was made for the MI transition in infinite dimensions where the self-energy of the Green function becomes independent of momentum.¹⁴ Several authors^{15–18} determined the self-energy (*i.e.*, an effective medium) self-consistently so as to be identical with the local self-energy of an impurity embedded in a medium. The theory, called dynamical mean-field theory (DMFT), can be traced back to a many-body coherent potential approximation (CPA) in disordered alloys¹⁹ and is equivalent to the dynamical CPA^{20,21} used in the theory of magnetism.²² The DMFT has clarified the MI transition in infinite dimensions. One of its new features is that it can describe both quasiparticle states near the Fermi level and the Mott-Hubbard incoherent bands.

In the DMFT as well as the dynamical CPA one usually deals with the temperature Green function. Therefore one needs to perform numerical analytic continuations at finite temperatures, which often causes numerical difficulties in particular at low temperatures. We recently proposed an alternative method which directly starts from the retarded Green function. The method, which is called the projection operator method CPA (PM-CPA),²³ has been shown to be equivalent to the dynamical CPA and the DMFT.²⁴ In the PM-CPA, the Liouville operator is approximated by an energy-dependent Liouvillean for an effective Hamiltonian with a coherent potential. The latter is determined by a self-consistent CPA condition. By solving an impurity problem embedded in a medium with use of the renormalized perturbation theory (RPT), we obtained an interpolation theory for the MI transition.

Although one can treat the excitations from the weak to the strong Coulomb interaction regime with use of the single-site theories mentioned above, the single-site approximation (SSA) neglects the intersite correlations which often play an important role in real systems such as the Cu oxides and Fe-pnictides high-temperature superconducting compounds. In fact, recent photoelectron spectroscopy found a pseudo gap^{25,26} and a kink structure^{27,28} in cuprates which can not be explained by a SSA.

Because of the reasons mentioned above, we have recently proposed a nonlocal theory of excitation spectra called the self-consistent projection operator method (SCPM).²⁹ It is based on the projection technique^{30,31} and the incremental cluster expansion method.^{32–34} In this theory, all the off-diagonal self-energy matrix elements are calculated by means of an incremental cluster expansion from a diagonal effective medium $\tilde{\Sigma}_{ii\sigma}(z)$. The latter is determined by the CPA condition. We call this method here and in the following the SCPM-0. The theory takes into account long-range intersite correlations, which are missing in the other nonlocal theories such as the dynamical cluster theory^{35,36} and the cluster DMFT.^{37,38} Moreover, the theory can describe the momentum dependent excitation spectrum with high resolution because it is based on the retarded Green function and because the intersite correlations are taken into account up to infinity at each order of the incremental cluster expansion. Using the

SCPM-0, we investigated the excitation spectra of the Hubbard model on the simple cubic lattice²⁹ and the square lattice.^{39–41} Especially in the two-dimensional system, we found a marginal Fermi liquid behavior³⁹ and a kink structure^{40,41} in the quasiparticle state in the underdoped region. The former was proposed in a phenomenological theory⁴² and the latter was found in the photoemission experiments in cuprates.^{27,28}

The SCPM-0 makes use of a diagonal effective medium to describe the on-site correlations at surrounding sites. The self-consistency between the self-energy and the medium is achieved only for the diagonal site. Such a treatment results in a limited range of applications. In this paper, we extend the SCPM-0 by introducing a new off-diagonal effective medium $\tilde{\Sigma}_{ij\sigma}(z)$. All calculated off-diagonal self-energy matrix elements are consistent with all those of the medium. Such a full self-consistent projection operator method (FSCPM) should allow for an improved quantitative description of nonlocal excitations in solids, and should play an important role in the phenomena with long-range charge and spin fluctuations, in particular, in low dimensional systems.

In the following subsection 2.1, we briefly review the retarded Green function and projection technique. In the §2.2, we introduce an energy-dependent Liouville operator whose corresponding Hamiltonian consists of the noninteracting Hamiltonian and an off-diagonal effective medium. We then expand the nonlocal self-energy embedded in the off-diagonal effective medium using the incremental cluster method. In order to obtain the different terms of the expansion, we need to calculate cluster memory functions for the medium. In §2.3 we obtain them by making use of the renormalized perturbation scheme. The off-diagonal medium is determined by a fully self-consistent condition. We present in §3 numerical results for momentum dependent excitation spectra for the Hubbard model on a simple cubic lattice at half-filling, and demonstrate that the full self-consistency extends the range of application from the intermediate Coulomb interaction regime to the strongly correlated regime. Calculated spectra modify the previous results based on the SCPM-0 so as to suppress the nonlocal effects in the intermediate regime. In the strong Coulomb interaction regime, we find the shadow bands associated with strong antiferromagnetic (AF) correlations and the band splitting in the Mott-Hubbard incoherent bands. In the last section we summarize the numerical results and discuss future problems.

2. Full Self-Consistent Projection Operator Method

2.1 Retarded Green function and projection technique

We adopt the tight-binding Hubbard model consisting of the Hartree-Fock independent particle Hamiltonian H_0 and the residual interactions with intraatomic Coulomb interaction parameter U as follows:

$$H = H_0 + U \sum_i \delta n_{i\uparrow} \delta n_{i\downarrow} , \quad (1)$$

$$H_0 = \sum_{i,\sigma} \epsilon_\sigma n_{i\sigma} + \sum_{i,j,\sigma} t_{ij} a_{i\sigma}^\dagger a_{j\sigma} . \quad (2)$$

Here $\epsilon_\sigma = \epsilon_0 - \mu + U \langle n_{i-\sigma} \rangle$ is the Hartree-Fock atomic level. Note that $\langle \dots \rangle$ denotes a thermal average. The quantities ϵ_0 , μ , and t_{ij} are the atomic level, the chemical potential, and the transfer integral between sites i and j , respectively. Furthermore $a_{i\sigma}^\dagger$ ($a_{i\sigma}$) denotes the creation (annihilation) operator for an electron with spin σ on site i , while $n_{i\sigma} = a_{i\sigma}^\dagger a_{i\sigma}$ is the electron density operator for spin σ , and $\delta n_{i\sigma} = n_{i\sigma} - \langle n_{i\sigma} \rangle$.

The excitation spectra for electrons are obtained from a retarded Green function defined by

$$G_{ij\sigma}(t-t') = -i\theta(t-t') \langle [a_{i\sigma}(t), a_{j\sigma}^\dagger(t')]_+ \rangle . \quad (3)$$

Here $\theta(t)$ is the step function, $a_{i\sigma}(t)$ is the Heisenberg representation of $a_{i\sigma}$ defined by $a_{i\sigma}(t) = \exp(iHt) a_{i\sigma} \exp(-iHt)$. Furthermore, $[,]_+$ denotes the anti-commutator between the operators.

The Fourier representation of the retarded Green function is written as follows.¹

$$G_{ij\sigma}(z) = \left(a_{i\sigma}^\dagger \left| \frac{1}{z-L} a_{j\sigma}^\dagger \right. \right) . \quad (4)$$

Here the inner product between the operators A and B is defined by $(A|B) = \langle [A^+, B]_+ \rangle$. Also $z = \omega + i\delta$ with δ being an infinitesimal positive number, and L is a Liouville operator defined by $LA = [H, A]$ for an operator A . Note that $[,]$ is the commutator between the operators.

Using the projection technique, we obtain the Dyson equation for the retarded Green function as

$$G_{ij\sigma}(z) = [(z - \mathbf{H}_0 - \mathbf{\Lambda}(z))^{-1}]_{ij\sigma} . \quad (5)$$

Here the matrices are defined by $(\mathbf{H}_0)_{ij\sigma} = \epsilon_\sigma \delta_{ij} + t_{ij}$, and

$$\mathbf{\Lambda}_{ij\sigma}(z) = (\mathbf{\Lambda}(z))_{ij\sigma} = U^2 \bar{G}_{ij\sigma}(z) . \quad (6)$$

The reduced memory function $\bar{G}_{ij\sigma}(z)$ is defined by

$$\bar{G}_{ij\sigma}(z) = \left(A_{i\sigma}^\dagger \left| \frac{1}{z-\bar{L}} A_{j\sigma}^\dagger \right. \right) . \quad (7)$$

The operator $A_{i\sigma}^\dagger$ is given by

$$A_{i\sigma}^\dagger = a_{i\sigma}^\dagger \delta n_{i-\sigma} , \quad (8)$$

and the Liouville operator \bar{L} acting on $A_{j\sigma}^\dagger$ is defined by $\bar{L} = QLQ$, Q being $Q = 1 - P$. The projection operator P projects onto the original operator space $\{|a_{i\sigma}^\dagger\rangle\}$,

$$P = \sum_{i\sigma} |a_{i\sigma}^\dagger\rangle \langle a_{i\sigma}^\dagger| . \quad (9)$$

In a crystalline system, the Green function $G_{ij\sigma}(z)$ is obtained from its momentum rep-

resentation $G_{k\sigma}(z)$ as

$$G_{ij\sigma}(z) = \frac{1}{N} \sum_k G_{k\sigma}(z) \exp(i\mathbf{k} \cdot (\mathbf{R}_i - \mathbf{R}_j)) . \quad (10)$$

Here N is a number of site. The momentum-dependent Green function is given by

$$G_{k\sigma}(z) = \frac{1}{z - \epsilon_{k\sigma} - \Lambda_{k\sigma}(z)} . \quad (11)$$

Here $\epsilon_{k\sigma} = \epsilon_\sigma + \epsilon_k$ is the Hartree-Fock one-electron energy eigenvalue, ϵ_k is the Fourier transform of t_{ij} , and

$$\Lambda_{k\sigma}(z) = \sum_j \Lambda_{j0\sigma}(z) \exp(i\mathbf{k} \cdot \mathbf{R}_j) . \quad (12)$$

It should be noted that the momentum-dependent excitation spectrum is obtained from

$$\rho_{k\sigma}(\omega) = -\frac{1}{\pi} \text{Im} G_{k\sigma}(z) . \quad (13)$$

The local density of states (DOS) is given by

$$\rho_{i\sigma}(\omega) = -\frac{1}{\pi} \text{Im} G_{ii\sigma}(z) . \quad (14)$$

which is identical with the average DOS per atom, $\rho_\sigma(\omega) = 1/N \sum_k \rho_{k\sigma}(\omega)$ when all sites are equivalent to each other.

2.2 Incremental cluster expansion in the off-diagonal effective medium

In the full self-consistent projection method, we introduce an energy-dependent Liouville operator $\tilde{L}(z)$. Its corresponding Hamiltonian is that of an off-diagonal effective medium $\tilde{\Sigma}_{ij\sigma}(z)$. It is

$$\tilde{L}(z)A = [\tilde{H}_0(z), A] , \quad (15)$$

for arbitrary operator A and

$$\tilde{H}_0(z) = H_0 + \sum_{ij\sigma} \tilde{\Sigma}_{ij\sigma}(z) a_{i\sigma}^\dagger a_{j\sigma} . \quad (16)$$

Defining an interaction Liouville operator $L_1(z)$ such that

$$L_1(z)A = [H_1(z), A] , \quad (17)$$

with

$$H_1(z) = U \sum_i \delta n_{i\uparrow} \delta n_{i\downarrow} - \sum_{ij\sigma} \tilde{\Sigma}_{ij\sigma}(z) a_{i\sigma}^\dagger a_{j\sigma} , \quad (18)$$

we can rewrite the original Liouville operator L as follows.

$$L = \tilde{L}(z) + L_1(z) . \quad (19)$$

It should be noted that the interaction $H_1(z)$ contains the off-diagonal components $\tilde{\Sigma}_{ij\sigma}(z)$ ($i \neq j$) in addition to the diagonal ones $\tilde{\Sigma}_{ii\sigma}(z)$. Accordingly, we divide here the interaction Liouvillean $L_1(z)$ into single-site terms and pair-site ones. Furthermore we intro-

duce site-dependent prefactors $\{\nu_i\}$ which are either 1 or 0.

$$L_I(z) = \sum_i \nu_i \mathcal{L}_1^{(i)}(z) + \sum_{(i,j)} \nu_i \nu_j \mathcal{L}_1^{(ij)}(z) , \quad (20)$$

$$\mathcal{L}_I^{(i)}(z)A = \left[U \delta n_{i\uparrow} \delta n_{i\downarrow} - \sum_{\sigma} \tilde{\Sigma}_{ii\sigma}(z) n_{i\sigma} , A \right] , \quad (21)$$

$$\mathcal{L}_I^{(ij)}(z)A = \left[- \sum_{\sigma} (\tilde{\Sigma}_{ij\sigma}(z) a_{i\sigma}^{\dagger} a_{j\sigma} + \tilde{\Sigma}_{ji\sigma}(z) a_{j\sigma}^{\dagger} a_{i\sigma}) , A \right] . \quad (22)$$

After substituting the Liouvillean (19) into Eq. (7), we can expand the resolvent $(z - \bar{L})^{-1}$ with respect to $L_I(z)$ as follows.

$$(z - \bar{L})^{-1} = \bar{G}_0 + \bar{G}_0 T \bar{G}_0 , \quad (23)$$

$$T = \bar{L}_I + \bar{L}_I \bar{G}_0 \bar{L}_I + \bar{L}_I \bar{G}_0 \bar{L}_I \bar{G}_0 \bar{L}_I + \cdots . \quad (24)$$

Here $\bar{G}_0 = (z - \bar{L}_0(z))^{-1}$ and $\bar{L}_0(z) = Q \tilde{L}(z) Q$, while $\bar{L}_I(z) = Q L_I(z) Q$.

The T matrix operator may be expanded with respect to different sites as

$$T = \sum_i \nu_i T_i + \sum_{(i,j)} \nu_i \nu_j T_{ij} + \sum_{(i,j,k)} \nu_i \nu_j \nu_k T_{ijk} + \cdots . \quad (25)$$

The single-site T_i , two-site T_{ij} , and three-site T_{ijk} matrix scattering operators are obtained by setting the indices as $(\nu_i = 1, \nu_{l(\neq i)} = 0)$, $(\nu_i = \nu_j = 1, \nu_{l(\neq i,j)} = 0)$, $(\nu_i = \nu_j = \nu_k = 1, \nu_{l(\neq i,j,k)} = 0)$, and so on. It is

$$T_i = T^{(i)} , \quad (26)$$

$$T_{ij} = T^{(ij)} - T_i - T_j , \quad (27)$$

$$T_{ijk} = T^{(ijk)} - T_{ij} - T_{jk} - T_{ki} - T_i - T_j - T_k . \quad (28)$$

The operator $T^{(c)}$ ($c = i, ij, ijk, \dots$) at the right-hand-side (r.h.s.) of the above equations is the T matrix operators for the cluster c , *i.e.*,

$$T^{(c)} = \bar{L}_I^{(c)} (1 - \bar{G}_0 \bar{L}_I^{(c)})^{-1} . \quad (29)$$

Here $\bar{L}_I^{(c)} = Q L_I^{(c)}(z) Q$ and $L_I^{(c)}(z)$ is the interaction Liouvillean for a cluster c :

$$L_I^{(c)}(z) = \sum_{i \in c} \mathcal{L}_1^{(i)}(z) + \sum_{(i,j) \in c} \mathcal{L}_1^{(ij)}(z) . \quad (30)$$

Note that the sums in the above equation are taken over the sites or pairs belonging to the cluster c .

Substituting Eq. (25) into Eq. (23) we have

$$\bar{G}_{ij\sigma}(z, \{\nu_l\}) = \left(A_{i\sigma}^{\dagger} \left| \left(\bar{G}_0 + \sum_l \nu_l \bar{G}_0 T_l \bar{G}_0 + \sum_{(l,m)} \nu_l \nu_m \bar{G}_0 T_{lm} \bar{G}_0 + \cdots \right) A_{j\sigma}^{\dagger} \right. \right) . \quad (31)$$

In the incremental method,³²⁻³⁴ we first consider the self-energy contribution due to intra-atomic excitations, *i.e.*,

$$\overline{G}_{ii\sigma}^{(i)}(z) = \overline{G}_{ii\sigma}(z, \nu_i = 1, \nu_{l(\neq i)} = 0) = (A_{i\sigma}^\dagger | (\overline{G}_0 + \overline{G}_0 T_i \overline{G}_0) A_{i\sigma}^\dagger) . \quad (32)$$

Next we consider the scattering contribution due to a two-site increment in Eq. (31),

$$\overline{G}_{ii\sigma}^{(il)}(z) = \overline{G}_{ii\sigma}(z, \nu_i = \nu_l = 1, \nu_{m(\neq i,l)} = 0) = \overline{G}_{ii\sigma}^{(i)}(z) + (A_{i\sigma}^\dagger | \overline{G}_0 (T_l + T_{li}) \overline{G}_0 | A_{i\sigma}^\dagger) . \quad (33)$$

This defines two-site increment to the diagonal matrix element as

$$\Delta \overline{G}_{ii\sigma}^{(il)}(z) = \overline{G}_{ii\sigma}^{(il)}(z) - \overline{G}_{ii\sigma}^{(i)}(z) . \quad (34)$$

In the same way, we consider

$$\overline{G}_{ii\sigma}^{(ilm)}(z) = \overline{G}_{ii\sigma}^{(i)}(z) + \Delta \overline{G}_{ii\sigma}^{(il)}(z) + \Delta \overline{G}_{ii\sigma}^{(im)}(z) + (A_{i\sigma}^\dagger | \overline{G}_0 (T_{lm} + T_{ilm}) \overline{G}_0 | A_{i\sigma}^\dagger) . \quad (35)$$

Then, we define the increment for a three-site contribution.

$$\Delta \overline{G}_{ii\sigma}^{(ilm)}(z) = \overline{G}_{ii\sigma}^{(ilm)}(z) - \Delta \overline{G}_{ii\sigma}^{(il)}(z) - \Delta \overline{G}_{ii\sigma}^{(im)}(z) - \overline{G}_{ii\sigma}^{(i)}(z) . \quad (36)$$

The memory function $\overline{G}_{ii\sigma}(z)$ in Eq. (31) is then expanded as follows.

$$\overline{G}_{ii\sigma}(z) = \overline{G}_{ii\sigma}^{(i)}(z) + \sum_{l \neq i} \Delta \overline{G}_{ii\sigma}^{(il)}(z) + \frac{1}{2} \sum_{l \neq i} \sum_{m \neq i, l} \Delta \overline{G}_{ii\sigma}^{(ilm)}(z) + \dots . \quad (37)$$

It should be noted that $\overline{G}_{ii\sigma}^{(c)}(z)$ ($c = i, ij, \dots$) in Eqs. (32), (33), and (35) is obtained from the T -matrix $T^{(c)}$ given by Eq. (29) as

$$\overline{G}_{ij\sigma}^{(c)}(z) = (A_{i\sigma}^\dagger | (z - \overline{L}^{(c)}(z))^{-1} A_{j\sigma}^\dagger) . \quad (38)$$

Here the cluster Liouvillean $\overline{L}^{(c)}(z)$ is defined by

$$\overline{L}^{(c)}(z) = \overline{L}_0(z) + \overline{L}_1^{(c)}(z) . \quad (39)$$

In the same way, the off-diagonal memory function is obtained as follows.

$$\overline{G}_{ij\sigma}(z) = \overline{G}_{ij\sigma}^{(ij)}(z) + \sum_{l \neq i, j} \Delta \overline{G}_{ij\sigma}^{(ijl)}(z) + \frac{1}{2} \sum_{l \neq i, j} \sum_{m \neq i, j, l} \Delta \overline{G}_{ij\sigma}^{(ijlm)}(z) + \dots , \quad (40)$$

with

$$\Delta \overline{G}_{ij\sigma}^{(ijl)}(z) = \overline{G}_{ij\sigma}^{(ijl)}(z) - \overline{G}_{ij\sigma}^{(ij)}(z) , \quad (41)$$

$$\Delta \overline{G}_{ij\sigma}^{(ijlm)}(z) = \overline{G}_{ij\sigma}^{(ijlm)}(z) - \Delta \overline{G}_{ij\sigma}^{(ijl)}(z) - \Delta \overline{G}_{ij\sigma}^{(ijm)}(z) - \overline{G}_{ij\sigma}^{(ij)}(z) . \quad (42)$$

When we take into account all the terms on the r.h.s. of Eqs. (37) and (40), the memory function $\overline{G}_{ij\sigma}(z)$ does not depend on the effective medium $\tilde{\Sigma}_{ij\sigma}(z)$. However, it is not possible in general to calculate the terms up to higher orders; we have to truncate the incremental expansion at a certain stage. In that case the memory function $\overline{G}_{ij\sigma}(z)$ depends on the medium

$\tilde{\Sigma}_{ij\sigma}(z)$. We determine the latter from the following self-consistent equation,

$$\tilde{\Sigma}_{ij\sigma}(z) = \Lambda_{ij\sigma}(z) . \quad (43)$$

Note that the off-diagonal effective medium $\tilde{\Sigma}_{ij\sigma}(z)$ is the self-energy for the energy-dependent Liouvillean $\tilde{L}(z)$, *i.e.*, $\tilde{\Sigma}_{ij\sigma}(z) = U^2(A_{i\sigma}^\dagger |(z - \bar{L}_0(z))^{-1} A_{j\sigma}^\dagger) = U^2(A_{i\sigma}^\dagger |\bar{G}_0 A_{j\sigma}^\dagger)$. Thus the self-consistent equation (43) is equivalent to the condition that the T -matrix describing the scattering from the medium vanishes according to Eq. (23):

$$(A_{i\sigma}^\dagger |\bar{G}_0 T \bar{G}_0 A_{j\sigma}^\dagger) = 0 . \quad (44)$$

This is a generalization of the CPA.

The present theory reduces to the previous version of the nonlocal excitations (SCPM-0)²⁹ when the off-diagonal media $\tilde{\Sigma}_{ij\sigma}(z)$ ($i \neq j$) are omitted and only the self-consistency of the diagonal part is taken into account in Eq. (43). When in the SCPM-0 only the diagonal self-energy $\Lambda_{ii\sigma}(z)$ is taken into account (*i.e.*, when we make the SSA), the result reduces to the PM-CPA which we previously proposed.²³

2.3 Renormalized perturbation scheme to cluster memory functions

The incremental cluster expansion scheme given in the last subsection can be performed when the cluster memory function $\bar{G}_{ij\sigma}^{(c)}(z)$ defined by Eq. (38) is known. We obtain here an explicit expression for it. The Hamiltonian $H^{(c)}(z)$ to the cluster Liouvillean $L^{(c)}(z)$ in (38) is given by

$$H^{(c)} = H_0 + \sum_{ij\sigma} \tilde{\Sigma}_{ij\sigma}(z) a_{i\sigma}^\dagger a_{j\sigma} - \sum_{ij \in c} \sum_{\sigma} \tilde{\Sigma}_{ij\sigma}(z) a_{i\sigma}^\dagger a_{j\sigma} + U \sum_{i \in c} \delta n_{i\uparrow} \delta n_{i\downarrow} . \quad (45)$$

Introducing parameters $\lambda_{ij\sigma}$ ($0 \leq \lambda_{ij\sigma} \leq 1$), we can divide the Hamiltonian $H^{(c)}$ as

$$H^{(c)}(z) = \tilde{H}^{(c)}(z) + H_1^{(c)}(z) , \quad (46)$$

$$\tilde{H}^{(c)}(z) = H_0 + \sum_{ij\sigma} \tilde{\Sigma}_{ij\sigma}(z) a_{i\sigma}^\dagger a_{j\sigma} - \sum_{ij \in c} \sum_{\sigma} \bar{\lambda}_{ij\sigma} \tilde{\Sigma}_{ij\sigma}(z) a_{i\sigma}^\dagger a_{j\sigma} , \quad (47)$$

$$H_1^{(c)}(z) = U \sum_{i \in c} \delta n_{i\uparrow} \delta n_{i\downarrow} - \sum_{ij \in c} \sum_{\sigma} \lambda_{ij\sigma} \tilde{\Sigma}_{ij\sigma}(z) a_{i\sigma}^\dagger a_{j\sigma} . \quad (48)$$

Here $\bar{\lambda}_{ij\sigma} = 1 - \lambda_{ij\sigma}$. Note that parameters $\lambda_{ij\sigma}$ control the partition ratio of the medium potentials $\tilde{\Sigma}_{ij\sigma}$ in the cluster between the noninteracting part $\tilde{H}^{(c)}(z)$ and the interacting part $H_1^{(c)}(z)$ (see Fig. 1). The Hamiltonian $\tilde{H}^{(c)}(z)$ denotes a system with a uniform effective medium $\tilde{\Sigma}_{ij\sigma}(z)$ when $\lambda_{ij\sigma} = 1$ ($i, j \in c$). When $\lambda_{ij\sigma} = 0$ ($i, j \in c$), $\tilde{H}^{(c)}(z)$ denotes a reference system with a cluster cavity in the effective medium and $H_1^{(c)}(z)$ denotes the Coulomb interactions on the cluster sites.

According to the partition of the Hamiltonian (46), we introduce a *noninteracting* Liou-

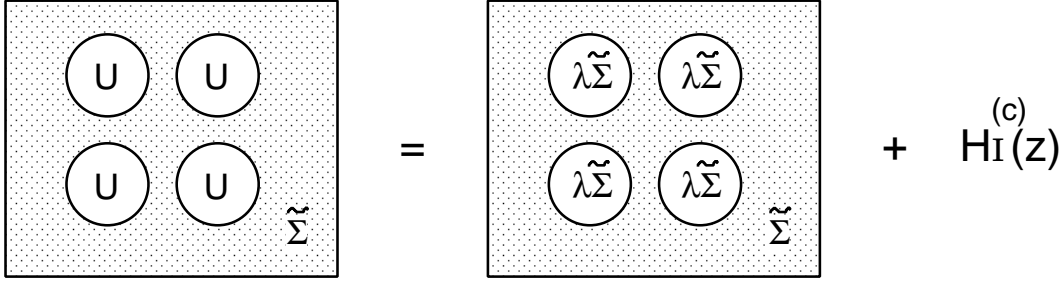


Fig. 1. Partition of the medium on the cluster sites. The cluster Hamiltonian $H^{(c)}(z)$ with on-site Coulomb interaction embedded in the off-diagonal medium $\tilde{\Sigma}$ (the left-hand-side) can be split into an effective Hamiltonian $\tilde{H}^{(c)}(z)$ with cluster potential $\lambda\tilde{\Sigma}$ and the remaining interaction $H_I^{(c)}(z)$. The parameter λ can control the magnitude of the potential $\tilde{\Sigma}$ on the cluster sites. Note that each site in the cluster may be away from the other sites of the cluster.

villean $\bar{L}_0^{(c)}(z) = QL_0^{(c)}(z)Q$ and an *interacting* Liouvillean $\bar{L}_I^{(c)}(z) = QL_I^{(c)}(z)Q$ as follows.

$$L_0^{(c)}(z)A = [\tilde{H}^{(c)}(z), A], \quad (49)$$

$$L_I^{(c)}(z)A = [H_I^{(c)}(z), A]. \quad (50)$$

Then we have $L^{(c)}(z) = L_0^{(c)}(z) + L_I^{(c)}(z)$, and the cluster memory function $\bar{G}_{ij\sigma}^{(c)}(z)$ is expressed as

$$\bar{G}_{ij\sigma}^{(c)}(z) = (A_{i\sigma}^\dagger | (z - \bar{L}_0^{(c)}(z) - \bar{L}_I^{(c)}(z))^{-1} A_{j\sigma}^\dagger). \quad (51)$$

Note that $\bar{L}_I^{(c)}(z)$ in the above expression has been redefined by Eq. (50), *i.e.*, Eq. (30) in which $\tilde{\Sigma}_{ij\sigma}(z)$ has been replaced by $\lambda_{ij\sigma}\tilde{\Sigma}_{ij\sigma}(z)$.

The interaction Liouvillean $\bar{L}_I^{(c)}(z)$ expands the operator space to

$$\bar{L}_I^{(c)}(z)|A_{l\sigma}^\dagger) = \left[U(1 - 2\langle n_{l-\sigma} \rangle) - \lambda_{l\sigma}\tilde{\Sigma}_{ll\sigma}(z) \right] |A_{l\sigma}^\dagger) - \sum_{(i,j) \in c} \left(\delta_{lj} |\tilde{B}_{li\sigma}^\dagger) + \delta_{li} |\tilde{B}_{lj\sigma}^\dagger) \right), \quad (52)$$

$$\begin{aligned} |\tilde{B}_{lj\sigma}^\dagger) &= \lambda_{lj\sigma}\tilde{\Sigma}_{lj\sigma}(z)|a_{j\sigma}^\dagger \delta n_{l-\sigma}) \\ &+ \lambda_{lj-\sigma}\tilde{\Sigma}_{lj-\sigma}(z)|a_{l\sigma}^\dagger \delta(a_{j-\sigma}^\dagger a_{l-\sigma}) + \lambda_{lj-\sigma}\tilde{\Sigma}_{lj-\sigma}(z)|a_{l\sigma}^\dagger \delta(a_{l-\sigma}^\dagger a_{j-\sigma})). \end{aligned} \quad (53)$$

Therefore we introduce the projection operator

$$\bar{P} = \sum_{i\sigma} |A_{i\sigma}^\dagger) \chi_{i\sigma}^{-1} (A_{i\sigma}^\dagger |, \quad (54)$$

where $\chi_{i\sigma} = \langle n_{i-\sigma} \rangle (1 - \langle n_{i-\sigma} \rangle)$. It projects onto the space $\{|A_{i\sigma}^\dagger)\}$, while $\bar{Q} = 1 - \bar{P}$ eliminates the space $\{|A_{i\sigma}^\dagger)\}$. Making use of these operators one can divide the interaction Liouvillean $\bar{L}_I^{(c)}(z)$ into two parts.

$$\bar{L}_I^{(c)}(z) = \bar{P} \bar{L}_I^{(c)}(z) \bar{P} + \bar{L}_{IQ}^{(c)}(z), \quad (55)$$

$$\overline{L}_{IQ}^{(c)}(z) = \overline{Q} \overline{L}_I^{(c)}(z) \overline{P} + \overline{L}_I^{(c)}(z) \overline{Q} . \quad (56)$$

The first term at the r.h.s. of Eq. (55) acts in the subspace $\{|A_{i\sigma}^\dagger\rangle\}$, while the second term expands the operator space beyond $\{|A_{i\sigma}^\dagger\rangle\}$. It should be noted that the first term at the r.h.s. of Eq. (56) does not vanish in general when we take into account the off-diagonal character of the effective medium. This point differs from the case of the SSA.²³

Making use of Eq. (52), we obtain the expression of $\overline{P} \overline{L}_I^{(c)}(z) \overline{P}$ in Eq. (55) as

$$\overline{P} \overline{L}_I^{(c)}(z) \overline{P} = \sum_{ij\sigma\sigma'} |A_{i\sigma}^\dagger\rangle (\overline{L}_I^{(c)})_{i\sigma j\sigma'} \langle A_{j\sigma'}^\dagger| , \quad (57)$$

$$\begin{aligned} (\overline{L}_I^{(c)})_{i\sigma j\sigma'} &= \frac{[U(1 - 2\langle n_{i-\sigma} \rangle) - \lambda_{i\sigma} \tilde{\Sigma}_{i\sigma}(z)] \delta_{\sigma\sigma'} - \chi_{i\sigma}^{-1} \sum_{l(\neq i) \in c} (A_{i\sigma}^\dagger | \tilde{B}_{il\sigma'}^\dagger) \delta_{ij}}{\chi_{i\sigma}} \delta_{ij} \\ &\quad - \frac{(A_{j\sigma}^\dagger | \tilde{B}_{j\sigma'}^\dagger)}{\chi_{i\sigma} \chi_{j\sigma'}} (1 - \delta_{ij}) . \end{aligned} \quad (58)$$

Substituting Eq. (55) into Eq. (51), we obtain

$$\overline{G}_{ij\sigma}^{(c)}(z) = \left[\overline{G}_0^{(c)} \cdot (1 - \overline{L}_I^{(c)} \cdot \overline{G}_0^{(c)})^{-1} \right]_{ij\sigma} . \quad (59)$$

Here the screened memory function $\overline{G}_{0ij\sigma}^{(c)}(z) = (\overline{G}_0^{(c)})_{i\sigma j\sigma}$ is defined by

$$\overline{G}_{0ij\sigma}^{(c)}(z) = (A_{i\sigma}^\dagger | (z - \overline{L}_0(z) - \overline{L}_{IQ}^{(c)}(z))^{-1} A_{j\sigma}^\dagger) . \quad (60)$$

The expression of the cluster memory function (59) is exact. The simplest approximation is to neglect the interaction Liouville operator $\overline{L}_{IQ}^{(c)}$ in the screened cluster memory function $\overline{G}_{0ij\sigma}^{(c)}$, which we called the zeroth renormalized perturbation theory (RPT-0). The approximation yields in the weak interaction limit the correct result of second-order perturbation theory, as well as the exact atomic limit.

An explicit expression of the screened cluster memory function in the RPT-0 can be obtained approximately as shown in Appendix.

$$\overline{G}_{0ij\sigma}^{(c)}(z) = A_{ij\sigma} \int \frac{d\epsilon d\epsilon' d\epsilon'' \rho_{ij\sigma}^{(c)}(\lambda, \epsilon) \rho_{ij-\sigma}^{(c)}(\lambda, \epsilon') \rho_{ji-\sigma}^{(c)}(\lambda, \epsilon'') \chi(\epsilon, \epsilon', \epsilon'')}{z - \epsilon - \lambda_\sigma \tilde{\Sigma}_\sigma(\epsilon, z) - \epsilon' - \lambda_{-\sigma} \tilde{\Sigma}_{-\sigma}(\epsilon', z) + \epsilon'' + \lambda_{-\sigma} \tilde{\Sigma}_{-\sigma}(\epsilon'', z)} , \quad (61)$$

$$\chi(\epsilon, \epsilon', \epsilon'') = (1 - f(\epsilon))(1 - f(\epsilon'))f(\epsilon'') + f(\epsilon)f(\epsilon')(1 - f(\epsilon'')) . \quad (62)$$

Here $0 \leq \lambda_\sigma \leq 1$, and $f(\omega)$ is the Fermi distribution function.

The prefactor $A_{ij\sigma}$ in Eq. (61) has been introduced to recover the exact second moment of the spectrum.

$$A_{ij\sigma} = \frac{\chi_{i\sigma}}{\langle n_{i-\sigma} \rangle_c (1 - \langle n_{i-\sigma} \rangle_c)} \delta_{ij} + 1 - \delta_{ij} . \quad (63)$$

Here the electron number for a cavity state $\langle n_{i\sigma} \rangle_c$ is defined by

$$\langle n_{i\sigma} \rangle_c = \int d\epsilon \rho_{i\sigma}^{(c)}(\lambda, \epsilon) f(\epsilon) . \quad (64)$$

The densities of states for the cavity state are given by

$$\rho_{ij\sigma}^{(c)}(\lambda, \epsilon) = -\frac{1}{\pi} \text{Im} [(\mathbf{F}_c(\lambda, z)^{-1} + \bar{\lambda}_\sigma \tilde{\Sigma}^{(c)}(z))^{-1}]_{ij\sigma}, \quad (65)$$

$$(\mathbf{F}_c(\lambda, z))_{ij\sigma} = F_{ij\sigma}(z) = \sum_k \frac{\langle i|k\rangle \langle k|j\rangle}{z - \epsilon_{k\sigma} - \bar{\lambda}_\sigma \tilde{\Sigma}_{k\sigma}(z)}. \quad (66)$$

Furthermore, $\bar{\lambda}_\sigma = 1 - \lambda_\sigma$, $(\tilde{\Sigma}^{(c)}(z))_{ij\sigma} = \tilde{\Sigma}_{ij\sigma}(z)$ ($i, j \in c$), and $\tilde{\Sigma}_{k\sigma}(z)$ is the Fourier transform of $\tilde{\Sigma}_{ij\sigma}(z)$; $\tilde{\Sigma}_{k\sigma}(z) = \sum_j \tilde{\Sigma}_{j0\sigma}(z) \exp(i\mathbf{k} \cdot \mathbf{R}_j)$.

The simplified self-energy $\tilde{\Sigma}_\sigma(\epsilon, z)$ in Eq. (61) is calculated from $\tilde{\Sigma}_{ij\sigma}(z)$ as

$$\tilde{\Sigma}_\sigma(\epsilon, z) = \sum_i \frac{\rho_{ij}^0(\epsilon - \epsilon_\sigma)}{\rho^0(\epsilon - \epsilon_\sigma)} \tilde{\Sigma}_{ij\sigma}(z), \quad (67)$$

where $\rho_{ij}^0(\epsilon)$ is the DOS of the noninteracting system defined by $\rho_{ij}^0(\epsilon) = \sum_k \langle i|k\rangle \delta(\epsilon - \epsilon_k) \langle k|j\rangle$ and $\rho^0(\epsilon)$ is defined by $\rho^0(\epsilon) = 1/N \sum_k \delta(\epsilon - \epsilon_k)$.

Finally the simplified cluster memory function in the RPT-0 is given by Eq. (59), Eq. (58) in which $\{\lambda_{ij\sigma}\}$ has been replaced by $\{\lambda_\sigma\}$, and Eq. (61). In the present scheme, we first assume $\tilde{\Sigma}_{ij\sigma}(z)$. Then we calculate the coherent Green function $F_{ij\sigma}(z)$ (Eq. (66)), the screened cluster memory function $\bar{G}_{0ij\sigma}^{(c)}(z)$ according to Eq. (61), as well as the atomic frequency matrix $(\bar{\mathbf{L}}_I^{(c)})_{ij\sigma\sigma'}$ given by Eq. (58). Using these matrices, we calculate the cluster memory function $\bar{G}_{ij\sigma}^{(c)}(z)$ (Eq. (59)). Note that the static quantities $(A_{i\sigma'}^\dagger | \tilde{B}_{j\sigma'}^\dagger)$ in Eq. (58) have to be calculated separately, for example, by means of the local ansatz wavefunction method.¹ After having calculated cluster memory functions, we can obtain the memory functions (37) and (40) according to the incremental scheme. Then we calculate the diagonal and off-diagonal self-energies (6). If the self-consistent condition (43) is not satisfied, we repeat the above-mentioned procedure renewing the medium $\tilde{\Sigma}_{ij\sigma}(z)$ until the self-consistency (43) is achieved. When we obtain the self-consistent solution $\tilde{\Sigma}_{ij\sigma}(z)$, we can calculate the excitation spectrum $\rho_{k\sigma}(\omega)$ from the Green function (11) and the DOS $\rho_\sigma(\omega)$ from Eq. (14).

3. Nonlocal Excitations on a Simple-Cubic Lattice

We present here the numerical results of excitation spectra of the Hubbard model on a simple cubic lattice at half-filling in the paramagnetic state in order to examine the nonlocal correlations in the FSCPM. As in our previous calculations, we choose the parameters $\lambda_\sigma = 0$ in Eq. (61); we start from the cavity cluster state ($\lambda_{ij} = 0$) for the calculation of the memory function. The form (61) with $\lambda_\sigma = 0$ reduces to the iterative perturbation scheme⁴³ at half-filling in infinite dimensions. Note that we need not to calculate $\tilde{\Sigma}_\sigma(\epsilon, z)$ defined by Eq. (67) as well as $(A_{j\sigma}^\dagger | \tilde{B}_{i\sigma}^\dagger)$ in Eq. (58) when $\lambda_\sigma = 0$.

We adopt the nearest-neighbor transfer integral t here and in the following, choose the energy unit as $|t| = 1$. The Fourier transform of the transfer integrals is given by $\epsilon = -2(\cos k_x + \cos k_y + \cos k_z)$ in the unit of lattice constant a . Furthermore, in Eqs. (37) and

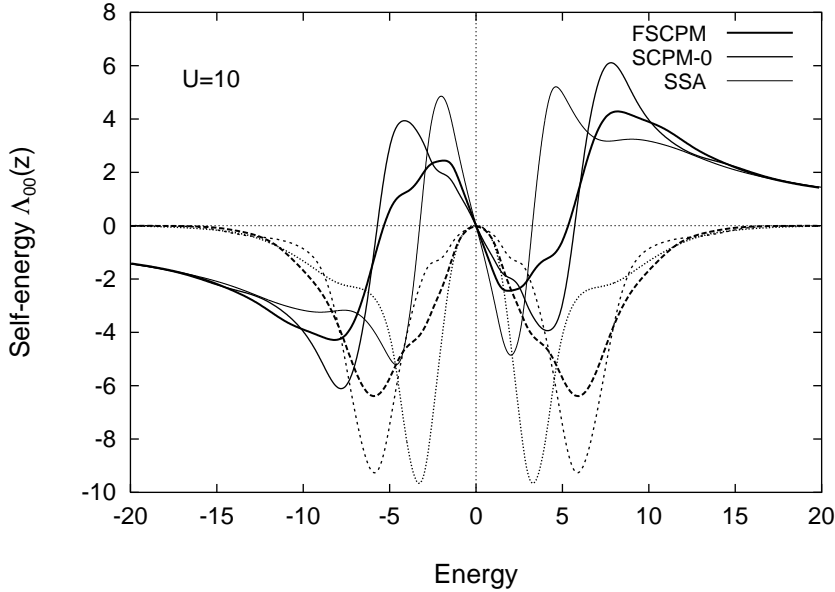


Fig. 2. Diagonal self-energies for $U = 10$ in the FSCPM (thick curves), the SCPM-0 (middle-size curves), and the SSA (thin curves). The real (imaginary) part in each method is drawn by the solid (dotted) curve.

(40) we take into account single-site and pair-site terms only, but the latter up to the 10th nearest neighbors. In the FSCPM, we have to perform a numerical k integration to obtain the coherent Green function $F_{ij\sigma}$ (see Eq. (66)). We have adopted a $80 \times 80 \times 80$ mesh in the first Brillouin zone for such integration.

In the numerical calculations of the screened memory function (61), we applied the method of Laplace transformation.⁴⁴ This reduces the 3-fold integrals with respect to energy into the one-fold integral with respect to time.

Starting from an initial set of values $\{\tilde{\Sigma}_{0j}(z) = 0\} (j = 0, 1, \dots, M)$, we calculated $\{F_{ij}(z)\}$ (Eq. (66)), $\{\rho_{ij}^{(c)}(z)\}$ (Eq. (65)), $\{\bar{G}_{0ij}^{(c)}(z)\}$ (Eq. (61)), $\{\bar{G}_{ij}^{(c)}(z)\}$ (Eq. (59)), and $\{\bar{G}_{ij}(z)\}$ (Eqs. (37) and (40)), and finally obtained $\Lambda_{ij\sigma}(z) = U^2 \bar{G}_{ij\sigma}(z)$. We have repeated the same procedure until self-consistency (43) was achieved.

We show in Fig. 2 the self-consistent diagonal self-energy at $U = 10$ and compare the results with the SSA and SCPM-0 calculations. The SCPM-0 shifts the spectral weight of the SSA towards the higher energy region. The FSCPM suppresses the amplitude of the SCPM-0 self-energy in the high energy region. In the low energy region, we find that the imaginary part is close to that of the SSA, while the real part is in-between the SSA and the SCPM-0.

The off-diagonal self-energies are shown in Fig. 3. We find again that self-energies are suppressed by the full self-consistency. Furthermore the self-energies rapidly damp with increasing interatomic distance. The fourth-nearest neighbor contribution and the contribution from more distant pairs can be neglected when $U = 10$, though we took into account the

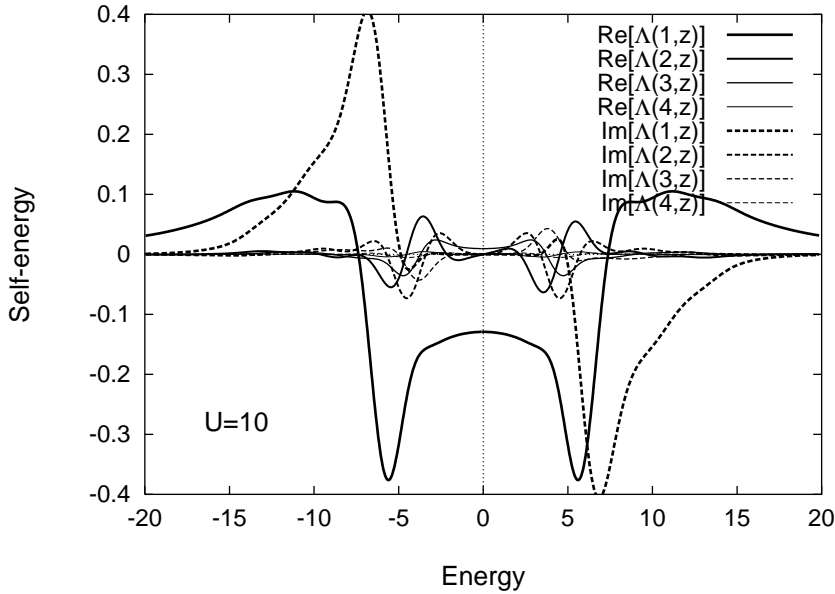


Fig. 3. Off-diagonal self-energy $\Lambda(n, z)$ for the n -th nearest neighbor pairs ($n = 1, 2, 3, 4$).

off-diagonal ones up to 10th nearest neighbors.

The momentum-dependent self-energies $\Lambda_{k\sigma}(z)$ are also suppressed by the full self-consistency. As shown in Fig. 4, in the low energy region the imaginary parts of $\Lambda_{k\sigma}(z)$ hardly depend on momentum \mathbf{k} and are close to those of the SSA. In the incoherent region $|\omega| \gtrsim 2$, both real and imaginary parts show considerable \mathbf{k} dependence. For example, the imaginary part of $\Lambda_{k\sigma}(z)$ shows at the Γ point a minimum at $\omega \approx 6$ and a second one at $\omega \approx -5$, while it shows a minimum at $\omega = -6$ and the second one at $\omega = 5$ at the R point.

Calculated momentum dependent excitation spectra are shown in Figs. 5, 6, and 7. For rather weak Coulomb interaction ($U = 6$), we find that the quasiparticle band is reduced by about 30% in width as compared with that of the noninteracting band. As seen in Fig. 5, the Mott-Hubbard incoherent bands appear at $|\omega| \approx 7.5$ around the Γ and R point. The spectral weight of the Mott-Hubbard bands is reduced by 30% when it is compared with that of the SCPM-0.

In the intermediate Coulomb interaction regime ($U = 10$), the quasiparticle band width becomes narrower and is reduced by 25% as compared with that of the SCPM-0. The spectral weight of the quasiparticle band around the Γ and R point moves farther to the lower and upper Mott-Hubbard bands. The latter are more localized in the vicinity of the Γ and R point than in the SCPM-0, and their peaks are reduced by 25% as compared with those in the SCPM-0.

In the FSCPM scheme, we can obtain the momentum-dependent spectra in the strong Coulomb interaction regime ($U = 16$). This is shown in Fig. 7. In this regime, the quasiparticle band becomes narrower and the spectral weight becomes smaller. New excitations which

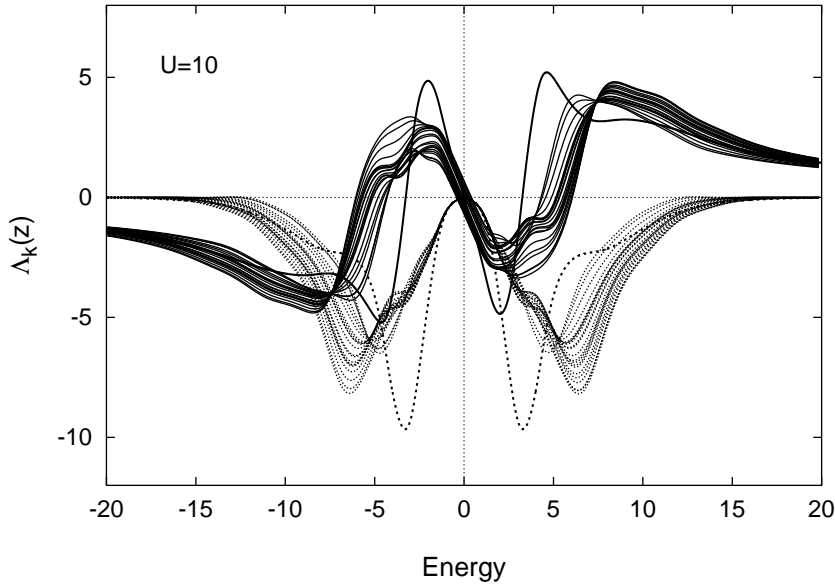


Fig. 4. Momentum dependent self-energies at various k points along the high symmetry line Γ -X-M-R. The real (imaginary) parts are shown by solid (dotted) curves. Note that the real part at the Γ point shows a maximum at energy $\omega \approx 8$ and a second maximum at $\omega \approx -3$, while the imaginary part shows a minimum at $\omega \approx 6$ and a second minimum at $\omega \approx -5$. The results of the SSA are also shown by the thick solid and dotted curves.

appear in this regime are the subbands at $|\omega| \approx 3.3$ showing weak momentum dependence. Because of the strong AF intersite correlations at half-filling, these excitations may be interpreted as “shadow” bands due to AF correlations, whose excitation spectra in a simple spin density wave (SDW) picture⁴⁵ may be given by $\epsilon_{\pm}^{SDW}(k) = \pm \sqrt{\tilde{\epsilon}_k^2 + \Delta^2}$. Here $\tilde{\epsilon}_k$ is a quasi-particle band, Δ is an exchange splitting defined by $\Delta = U_{\text{eff}}|m|/2$, $|m|$ being a temporal amplitude of the magnetic moments with long-range AF correlations, and U_{eff} is an effective Coulomb interaction.

As seen in Fig. 7 the Mott-Hubbard bands in the strong Coulomb interaction regime show a weak momentum dependence around $|\omega| \approx \pm 11$. It should be noted that the splitting between the upper and lower Hubbard bands is about 22, which is larger than $U = 16$ (a value yielding the atomic limit). In the strong Coulomb interaction limit at half-filling, we expect strong AF intersite correlations due to the super-exchange interaction $J = 4|t|^2/U$. The energy to remove (add) electrons is then expected to be $\epsilon_0 - z_{\text{NN}}|J|$ ($\epsilon_0 + U + z_{\text{NN}}|J|$), z_{NN} being the number of nearest neighbors ($z_{\text{NN}} = 6$ in the present case). Thus the splitting is expected to be $U + 2z_{\text{NN}}|J|$ instead of U . This formula yields the splitting 19 instead of $U = 16$. The former seems to be consistent with the value 22. We also find additional excitations at $|\omega| \approx 8$. These sub-bands may be interpreted as local excitations of the lower and upper Hubbard bands without AF correlations.

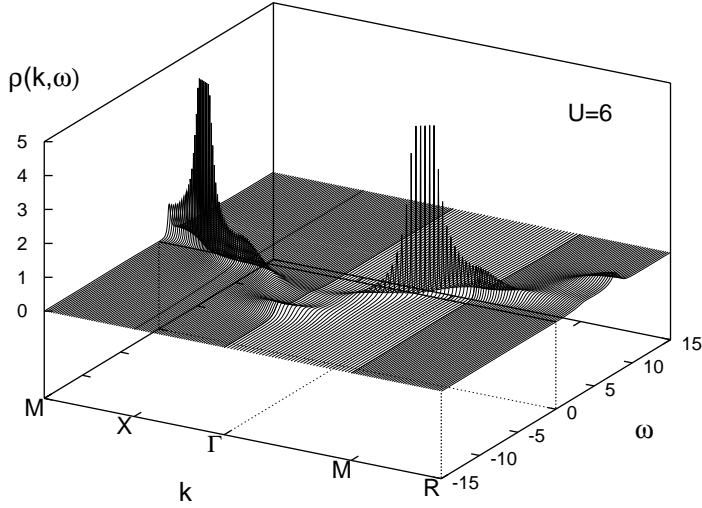


Fig. 5. Single-particle excitation spectra along the high-symmetry lines at $U = 6$. The Fermi level is indicated by a bold line.

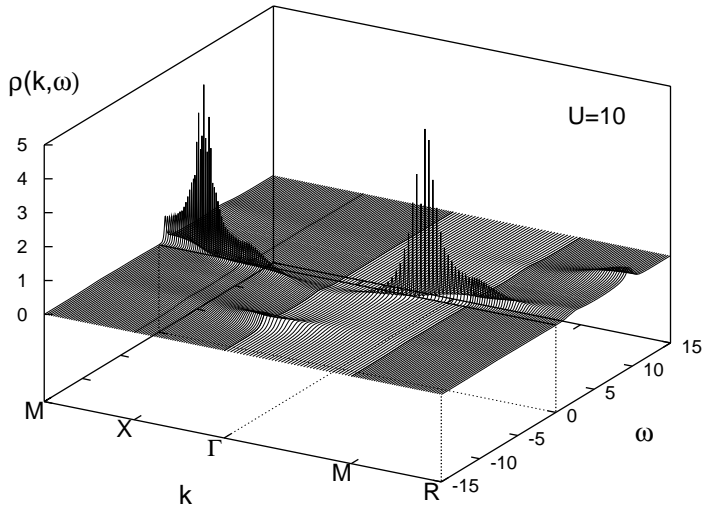


Fig. 6. Single-particle excitation spectra at $U = 10$.

The total densities of states are presented in Fig. 8 for various values of U . For weak Coulomb interactions $U \lesssim 6$, the deviation of the spectra from those of the SCPM-0 is negligible. When $U > 6$, Mott-Hubbard bands appear and the DOS deviate from the SCPM-0. An example is shown in Fig. 9 for $U = 10$. We find there that the full self-consistency suppresses the weight of the Mott-Hubbard bands and enhances the quasiparticle peaks.

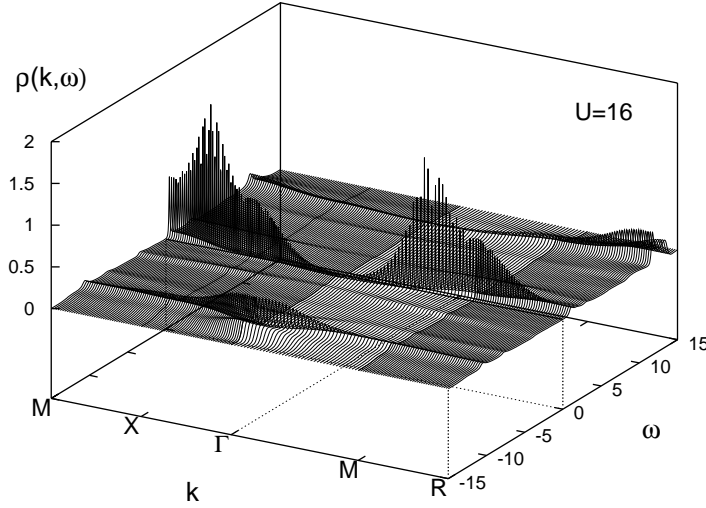


Fig. 7. Single-particle excitation spectra at $U = 16$. Note that the vertical scale has been changed in order to show detailed structure of excitations.

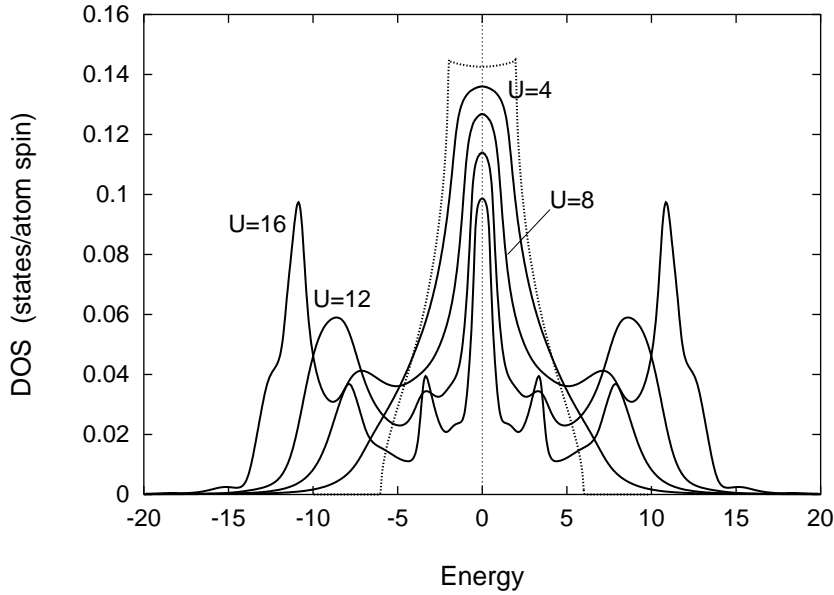


Fig. 8. The total DOS for $U = 4, 8, 12, 16$. The DOS for noninteracting system is shown by dotted curve.

Resulting DOS is in-between the SSA and the SCPM-0. When $U > 10$, a shadow band develops around $|\omega| = 3$ as seen in Fig. 8. Furthermore, for $U > 12$ we find two peaks in each Mott-Hubbard band; one is due to the excitations without intersite AF correlations, another is due to the excitations with strong AF correlations.

A remarkable point of the nonlocal excitation spectra is that the quasiparticle peak at the

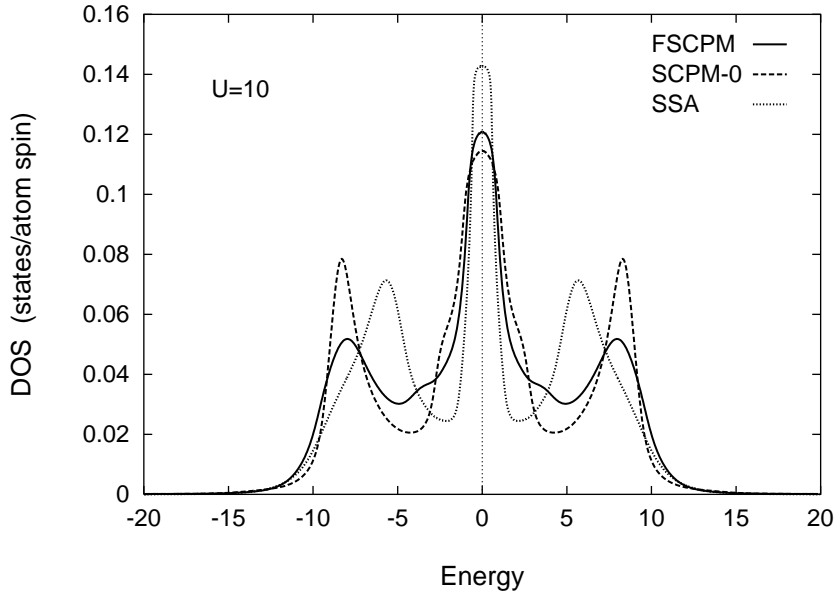


Fig. 9. The DOS in the FSCPM (solid curve), the SCPM-0 (dashed curve), and the SSA (dotted curve) at $U = 10$.

Fermi level reduces with increasing Coulomb interaction U . As shown in Fig 10, the ratio of $\rho(0)/\rho_{\text{SSA}}(0)$ to the SSA, monotonically decreases with increasing U , and reaches 0.59 when $U = 20$.

Momentum-dependent effective masses m_k along the high symmetry line are presented in Fig. 11. In the FSCPM calculations, we obtained the self-consistent m_k up to $U = 20$. We find that m_k are approximately equal to those in the SCPM-0 for $U \lesssim 6$. But, for $U > 6$, the FSCPM enhances the mass m_k as compared with those of the SCPM-0. Momentum dependence of m_k becomes larger with increasing U . The mass has a minimum (*e.g.*, 9.4 for $U = 20$) at $\Gamma(0, 0, 0)$ and R (π, π, π) points, and has a maximum (*e.g.*, 10.0 for $U = 20$) at $(\pi, \pi/2, 0)$.

The average quasiparticle weight $Z = (N^{-1} \sum_k m_k)^{-1}$ vs. U curve is shown in Fig. 10. Quasiparticle weight in the SSA monotonically decreases and vanishes for $U_c = 16.0$. The curve in the SCPM-0 deviates upwards from the SSA. The curve in the FSCPM deviates downwards from the SCPM-0 beyond $U \approx 5$, and is between the SSA and the SCPM-0. The present result suggests that the critical Coulomb interaction for the divergence of the effective mass is $U_c(m^* = \infty) \gtrsim 30$. We want to mention that for the Gutzwiller wave function a critical Coulomb interaction $U_c(m^* = \infty)$ exists only in infinite dimensions (*i.e.*, in the SSA).⁴⁶⁻⁴⁸

We have also calculated the momentum distribution as shown in Fig. 12. The distributions show a jump at the Fermi surface, and extend beyond the surface. The basic behavior of the distribution is similar to that in the SCPM-0. For $U \lesssim 6$, the curves $\langle n_k \rangle$ agree with those of the SCPM-0. When $U > 6$, the FSCPM reduces $\langle n_k \rangle$ of the SCPM-0 below the Fermi level, and

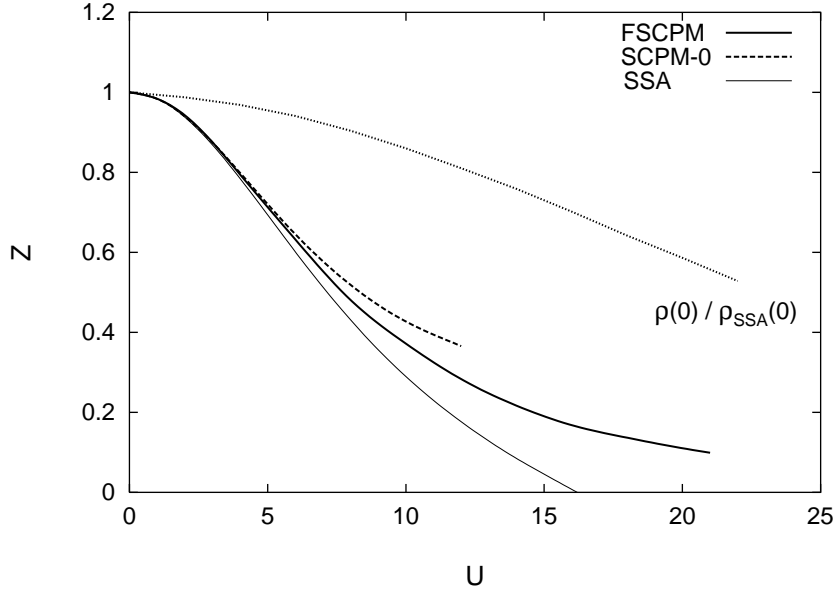


Fig. 10. The average quasiparticle weight vs. Coulomb interaction curves in the FSCPM (solid curves), the SCPM-0 (dashed curve), and the SSA (thin solid curve). The DOS divided by the SSA one at the Fermi level is shown by dotted curve. Note that $\rho_{\text{SSA}}(0)$ equals the noninteracting DOS $\rho^0(0)$. $\rho(0)/\rho_{\text{SSA}}(0)$ beyond $U_c(\text{SSA}) = 16.0$ stands for $\rho(0)/\rho^0(0)$.

enhances it above the Fermi level suggesting increased localization due to full self-consistency.

4. Summary and Discussions

We have developed a fully self-consistent projection operator method (FSCPM) for non-local excitations by using the projection technique for the retarded Green function and the effective medium. The method makes use of an energy-dependent Liouville operator $\tilde{L}(z)$ with a corresponding Hamiltonian for an off-diagonal effective medium $\tilde{\Sigma}_{ij\sigma}(z)$. It allows us to calculate the nonlocal self-energy $\Lambda_{ij\sigma}(z)$ by using the incremental cluster expansion from the off-diagonal medium. Each term of the expansion is calculated from the memory function for clusters in a nonlocal effective medium. The latters are obtained by the renormalized perturbation theory within the RPT-0. The off-diagonal effective medium $\tilde{\Sigma}_{ij\sigma}(z)$ is determined from a fully self-consistent condition $\{\tilde{\Sigma}_{ij\sigma}(z) = \Lambda_{ij\sigma}(z)\}$. It is a generalization of the CPA as given in Eq. (44), *i.e.*, $(A_{i\sigma}^\dagger | \overline{G}_0 T \overline{G}_0 A_{j\sigma}^\dagger) = 0$ where T denotes a scattering T -matrix from the off-diagonal medium and \overline{G}_0 is a resolvent for the Liouville operator \overline{L}_0 corresponding to the medium. In this way we can take into account the long-range intersite correlations as extensive as we want in each order of expansion. We obtain momentum-dependent spectra of high resolution from the weak to the strong Coulomb interaction regime.

The present theory reduces to the PM-CPA when we omit all off-diagonal matrix elements

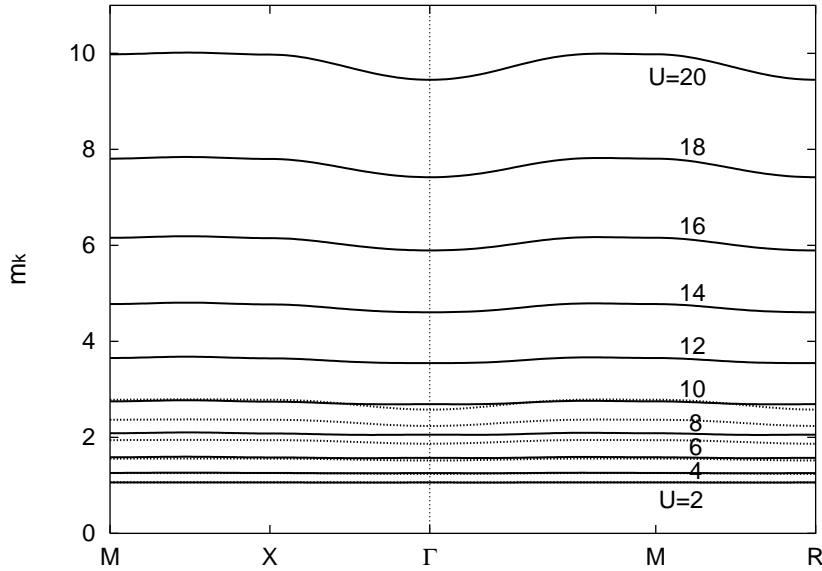


Fig. 11. The momentum-dependent effective mass curves along the high-symmetry lines for various Coulomb interaction U . The curves in the SCPM-0 are also shown by the dotted curves for $U = 2, 4, 6, 8, 10, \text{ and } 12$ from the bottom to the top.

of the effective medium $\tilde{\Sigma}_{ij\sigma}(z) (i \neq j)$ and all the off-diagonal self-energy contributions. The theory reduces to a self-consistent theory (SCPM-0) when we omit the off-diagonal medium $\tilde{\Sigma}_{ij\sigma}(z) (i \neq j)$, but take into account all the off-diagonal self-energy contribution $\Lambda_{ij\sigma}(z)$.

We have performed numerical calculations of the excitation spectra for the half-filled Hubbard model on a simple cubic lattice by using the FSCPM within the two-site approximation. We have obtained the self-consistent nonlocal self-energy up to the Coulomb interaction $U \approx 20$. We found that the FSCPM suppresses the amplitudes of local and nonlocal self-energy $\Lambda_{ij\sigma}(z)$ for an intermediate strength of Coulomb interactions, reduces the weight of the Mott-Hubbard bands, and enhances the quasiparticle peaks at the Fermi level in the average DOS when they are compared with those in the SCPM-0. Moreover the FSCPM enhances the momentum-dependent effective mass m_k as compared with the SCPM-0. Thus the $Z-U$ curve is located between the SSA and the SCPM-0. These results indicate that the full self-consistency tends to suppress the nonlocal effects found in the SCPM-0. We suggest a critical Coulomb interaction $U_c(m^* = \infty) \gtrsim 30$ for the simple cubic lattice, which is much larger than the SSA value $U_c = 16$. In order to obtain the explicit value of U_c , we have to take into account larger clusters embedded in the off-diagonal medium.

The FSCPM enables us to investigate the nonlocal excitation spectra in the strongly correlated region. There the quasiparticle bands becomes narrower and their weight becomes smaller. We found shadow band excitations at $|\omega| \approx 3$ due to strong AF correlations and Mott-Hubbard sub-bands at $|\omega| \approx U/2$ without intersite correlations. Moreover, we found

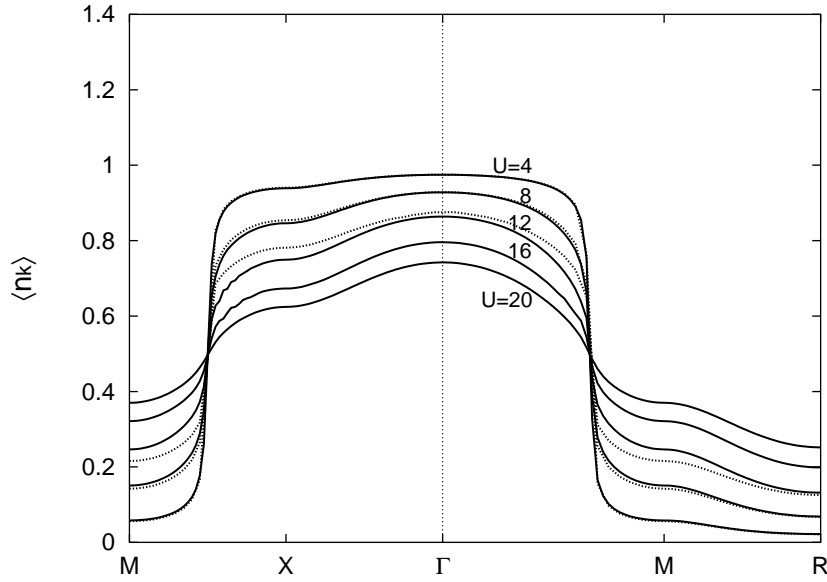


Fig. 12. Momentum distribution along the high-symmetry lines in the FSCPM (solid curves). The curves in the SCPM-0 are also drawn by dotted curves for $U = 4, 8, 12$.

that strong AF correlations can shift the Mott-Hubbard bands towards higher energies.

In the present calculations, we investigated the effects of nonlocal correlations assuming the paramagnetic state. One has to extend the calculations to the AF case in the next step because the ground state of the three dimensional Hubbard model is believed to be antiferromagnetic in general. Furthermore, the numerical results of calculations in the strongly correlated region presented here should be extended by taking into account the contributions from larger clusters in the incremental cluster expansion. Improvements of the self-energies for the clusters in the off-diagonal effective medium are also left for future investigations towards more quantitative calculations of the nonlocal excitations.

Acknowledgment

This work was supported by Grant-in-Aid for Scientific Research (19540408). Numerical calculations have been partly carried out with use of the Hitachi SR11000 in the Supercomputer Center, Institute of Solid State Physics, University of Tokyo.

Appendix: Derivation of Approximate Expression for the Screened Cluster Memory Function (61)

An approximate expression (61) of the screened cluster memory function in the RPT-0 can be obtained as follows by using the momentum representation of the operator space.

For that purpose, we first express the local operator $A_{i\sigma}^\dagger$ by means of the creation and annihilation operators in the momentum representation as

$$A_{i\sigma}^\dagger = \sum_{k,k',k''} a_{k\sigma}^\dagger \delta(a_{k'-\sigma}^\dagger a_{k''-\sigma}) \langle k|i \rangle \langle k'|i \rangle \langle i|k'' \rangle. \quad (\text{A}\cdot 1)$$

Here $\langle k|i \rangle = \langle i|k \rangle^* = 1/\sqrt{N} \exp(i\mathbf{k} \cdot \mathbf{R}_i)$. The operator $a_{k\sigma}^\dagger \delta(a_{k'-\sigma}^\dagger a_{k''-\sigma})$ in Eq. (A·1) is the eigen state of $\bar{L}_0(z) = Q\tilde{L}(z)Q$, *i.e.*,

$$\begin{aligned} \bar{L}_0(z) |a_{k\sigma}^\dagger \delta(a_{k'-\sigma}^\dagger a_{k''-\sigma})\rangle &= [\epsilon_\sigma + \epsilon_k + \tilde{\Sigma}_{k\sigma}(z) + \epsilon_{k'} + \tilde{\Sigma}_{k'-\sigma}(z) \\ &\quad - \epsilon_{k''} - \tilde{\Sigma}_{k''-\sigma}(z)] |a_{k\sigma}^\dagger \delta(a_{k'-\sigma}^\dagger a_{k''-\sigma})\rangle. \end{aligned} \quad (\text{A}\cdot 2)$$

Here $\tilde{\Sigma}_{k\sigma}(z)$ is the Fourier transform of $\tilde{\Sigma}_{ij\sigma}(z)$, which is defined by $\tilde{\Sigma}_{k\sigma}(z) = \sum_j \tilde{\Sigma}_{j0\sigma}(z) \exp(i\mathbf{k} \cdot \mathbf{R}_j)$.

Substituting Eq. (A·1) into the approximate expression $\bar{G}_{0ij\sigma}^{(c)}(z) = (A_{i\sigma}^\dagger | (z - \bar{L}_0(z))^{-1} A_{j\sigma}^\dagger)$ and making use of the relation (A·2), we reach the explicit expression of the screened cluster memory function in the RPT-0 as

$$\bar{G}_{0ij\sigma}^{(c)}(z) = \sum_{kk'k''k_1k'_1k''_1} \langle i|k_1 \rangle \langle i|k'_1 \rangle \langle k''_1|i \rangle \langle k_1''|i \rangle (\bar{\mathbf{G}}_0^{(c)})_{k_1k'_1k''_1\sigma kk'k''\sigma} \langle k|j \rangle \langle k'|j \rangle \langle j|k'' \rangle, \quad (\text{A}\cdot 3)$$

$$\bar{\mathbf{G}}_0^{(c)} = \chi(z - \bar{\mathbf{L}}_0 - \mathbf{v}_c)^{-1}, \quad (\text{A}\cdot 4)$$

$$(\chi)_{k_1k'_1k''_1\sigma'kk'k''\sigma} = (a_{k_1\sigma'}^\dagger \delta(a_{k'_1-\sigma'}^\dagger a_{k''_1-\sigma'}) | a_{k\sigma}^\dagger \delta(a_{k'-\sigma}^\dagger a_{k''-\sigma})), \quad (\text{A}\cdot 5)$$

$$\begin{aligned} (\bar{\mathbf{L}}_0)_{k_1k'_1k''_1\sigma'kk'k''\sigma} &= (\epsilon_\sigma + \epsilon_k + \tilde{\Sigma}_{k\sigma}(z) + \epsilon_{k'} + \tilde{\Sigma}_{k'-\sigma}(z) \\ &\quad - \epsilon_{k''} - \tilde{\Sigma}_{k''-\sigma}(z)) \delta_{k_1k} \delta_{k'_1k'} \delta_{k''_1k''} \delta_{\sigma\sigma'}, \end{aligned} \quad (\text{A}\cdot 6)$$

$$\begin{aligned} (\mathbf{v}_c)_{k_1k'_1k''_1\sigma'kk'k''\sigma} &= \sum_{lm \in c} \left[-\bar{\lambda}_{lm\sigma} \tilde{\Sigma}_{lm\sigma}(z) \langle k_1|l \rangle \langle m|k \rangle \delta_{k'_1k'} \delta_{k''_1k''} \right. \\ &\quad - \bar{\lambda}_{lm-\sigma} \tilde{\Sigma}_{lm-\sigma}(z) \langle k'_1|l \rangle \langle m|k' \rangle \delta_{k_1k} \delta_{k''_1k''} \\ &\quad \left. + \bar{\lambda}_{lm-\sigma} \tilde{\Sigma}_{lm-\sigma}(z) \langle k''_1|l \rangle \langle m|k''_1 \rangle \delta_{k_1k} \delta_{k'_1k'} \right] \delta_{\sigma\sigma'}. \end{aligned} \quad (\text{A}\cdot 7)$$

The screened memory function (A·3) depends on the choice of $\{\lambda_{ij\sigma}\}$. When we choose $\{\lambda_{ij\sigma} = 1\}$ and adopt the Hartree-Fock approximation when computing the static average in

Eq. (A·5), we have

$$\overline{G}_{0ij\sigma}^{(c)}(z) = \sum_{k,k',k''} \frac{\langle i|k\rangle\langle i|k'\rangle\langle k''|i\rangle\chi(\epsilon_{k\sigma}, \epsilon_{k'-\sigma}, \epsilon_{k''-\sigma})\langle k|j\rangle\langle k'|j\rangle\langle j|k''\rangle}{z - \epsilon_{k\sigma} - \tilde{\Sigma}_{k\sigma}(z) - \epsilon_{k'-\sigma} - \tilde{\Sigma}_{k'-\sigma}(z) + \epsilon_{k''-\sigma} + \tilde{\Sigma}_{k''-\sigma}(z)}, \quad (\text{A}\cdot 8)$$

$$\chi(\epsilon_k, \epsilon_{k'}, \epsilon_{k''}) = (1 - f(\epsilon_k))(1 - f(\epsilon_{k'}))f(\epsilon_{k''}) + f(\epsilon_k)f(\epsilon_{k'})(1 - f(\epsilon_{k''})). \quad (\text{A}\cdot 9)$$

Here $\epsilon_{k\sigma} = \epsilon_\sigma + \epsilon_k$ is the Hartree-Fock energy, $f(\omega)$ is the Fermi distribution function.

A way to simplify in Eq. (A·8) the three-fold sum with respect to k might be to introduce an approximate $\tilde{\Sigma}_{k\sigma}(z)$ whose k dependence has been projected onto the Hartree-Fock energy $\epsilon_{k\sigma}$, as follows.

$$\tilde{\Sigma}_\sigma(\epsilon_{k\sigma}, z) = \frac{\int d\mathbf{k}' \delta(\epsilon_{k\sigma} - \epsilon_{k'\sigma}) \tilde{\Sigma}_{k'\sigma}(z)}{\int d\mathbf{k}' \delta(\epsilon_{k\sigma} - \epsilon_{k'\sigma})}. \quad (\text{A}\cdot 10)$$

After the approximation $\tilde{\Sigma}_{k\sigma}(z) \approx \tilde{\Sigma}_\sigma(\epsilon_{k\sigma}, z)$, Eq. (A·8) is expressed as

$$\overline{G}_{0ij\sigma}^{(c)}(z) = \int \frac{d\epsilon d\epsilon' d\epsilon'' \rho_{ij\sigma}(\epsilon) \rho_{ij-\sigma}(\epsilon') \rho_{ji-\sigma}(\epsilon'') \chi(\epsilon, \epsilon', \epsilon'')}{z - \epsilon - \tilde{\Sigma}_\sigma(\epsilon, z) - \epsilon' - \tilde{\Sigma}_{-\sigma}(\epsilon', z) + \epsilon'' + \tilde{\Sigma}_{-\sigma}(\epsilon'', z)}. \quad (\text{A}\cdot 11)$$

Here $\rho_{ij\sigma}(\epsilon)$ is the Hartree-Fock density of states defined by $\rho_{ij\sigma}(\epsilon) = \sum_k \langle i|k\rangle \delta(\epsilon - \epsilon_{k\sigma}) \langle k|j\rangle$.

On the other hand, in the case of $\{\lambda_{ij\sigma} = 0\}$ (*i.e.*, $\{\bar{\lambda}_{ij\sigma} = 1\}$), it is not easy to obtain directly a simplified expression of Eq. (A·3) because \mathbf{v}_c remains. However, $H_1^{(c)}(z)$ in Eq. (48) becomes the Coulomb interaction in this case. The second-order perturbation of the temperature Green function yields then an approximate expression.

$$\overline{G}_{0ij\sigma}^{(c)}(z) = \int \frac{d\epsilon d\epsilon' d\epsilon'' \rho_{ij\sigma}^{(c)}(\epsilon) \rho_{ij-\sigma}^{(c)}(\epsilon') \rho_{ji-\sigma}^{(c)}(\epsilon'') \chi(\epsilon, \epsilon', \epsilon'')}{z - \epsilon - \epsilon' + \epsilon''}. \quad (\text{A}\cdot 12)$$

Here $\rho_{ij\sigma}^{(c)}(\epsilon)$ is the DOS for a cavity Green function for the Hamiltonian (47) with $\{\bar{\lambda}_{ij\sigma} = 1\}$.

Therefore we obtain a simplified expression of the screened cluster memory function, which is an interpolation between Eq. (A·11) for $\lambda_{ij\sigma} = 1$ and Eq. (A·12) for $\lambda_{ij\sigma} = 0$.

$$\overline{G}_{0ij\sigma}^{(c)}(z) = A_{ij\sigma} \int \frac{d\epsilon d\epsilon' d\epsilon'' \rho_{ij\sigma}^{(c)}(\lambda, \epsilon) \rho_{ij-\sigma}^{(c)}(\lambda, \epsilon') \rho_{ji-\sigma}^{(c)}(\lambda, \epsilon'') \chi(\epsilon, \epsilon', \epsilon'')}{z - \epsilon - \lambda_\sigma \tilde{\Sigma}_\sigma(\epsilon, z) - \epsilon' - \lambda_{-\sigma} \tilde{\Sigma}_{-\sigma}(\epsilon', z) + \epsilon'' + \lambda_{-\sigma} \tilde{\Sigma}_{-\sigma}(\epsilon'', z)}. \quad (\text{A}\cdot 13)$$

This is Eq. (61). The prefactor $A_{ij\sigma}$, the densities of states for the cavity states $\rho_{ij\sigma}^{(c)}(\lambda, \epsilon)$, and a simplified self-energy $\tilde{\Sigma}_\sigma(\epsilon, z)$ are given by Eqs. (63), (65), and (67), respectively.

References

- 1) P. Fulde, *Electron Correlations in Molecules and Solids* (Springer, Berlin, 1995).
- 2) Z.-X. Shen, D.S. Dessau: Phys. Rep. **253** (1995) 1.
- 3) M. Imada, A. Fujimori, Y. Tokura: Rev. Mod. Phys. **70** (1998) 1039.
- 4) J. Hubbard: Proc. Roy. Soc. (London) **A276** (1963) 238.
- 5) J. Hubbard: Proc. Roy. Soc. (London) **A281** (1964) 401.
- 6) M. Cyrot: J. Phys. (Paris) **33** (1972) 25.
- 7) D.R. Penn: Phys. Rev. Lett. **42** (1979) 921.
- 8) A. Liebsch: Phys. Rev. Lett. **43** (1979) 1431; Phys. Rev. B **23** (1981) 5203.
- 9) W.D. Lukas and P. Fulde: Z. Phys. B **48** (1982) 113.
- 10) K.W. Becker and W. Brenig: Z. Phys. B **79** (1990) 195.
- 11) P. Unger and P. Fulde: Phys. Rev. B **48** (1993) 16607.
- 12) P. Unger, J. Igarashi, and P. Fulde: Phys. Rev. B **50** (1994) 10485.
- 13) P. Fulde: Adv. in Phys. **51** (2002) 909.
- 14) W. Metzner and D. Vollhardt: Phys. Rev. Lett. **62** (1989) 324.
- 15) E. Müller-Hartmann: Z. Phys. B **74** (1989) 507.
- 16) M. Jarrell: Phys. Rev. Lett. **69** (1992) 168; M. Jarrell and H.R. Krishnamurthy: Phys. Rev. B **63** (2001) 125102.
- 17) A. Georges and G. Kotliar: Phys. Rev. B **45** (1992) 6479; A. Georges and W. Krauth: Phys. Rev. B **48** (1993) 7167.
- 18) A. Georges, G. Kotliar, W. Krauth, and M. J. Rosenberg: Rev. Mod. Phys. **68** (1996) 13.
- 19) S. Hirooka and M. Shimizu: J. Phys. Soc. Jpn. **43** (1977) 70.
- 20) Y. Kakehashi: Phys. Rev. B **45** (1992) 7196; J. Magn. Magn. Mater. **104-107** (1992) 677.
- 21) Y. Kakehashi: Phys. Rev. B **65** (2002) 184420.
- 22) Y. Kakehashi: Phys. Rev. B **66** (2002) 104428.
- 23) Y. Kakehashi and P. Fulde: Phys. Rev. B **69** (2004) 045101.
- 24) Y. Kakehashi: Adv. Phys. **53** (2004) 497.
- 25) D.S. Marshall, D.S. Dessau, A.G. Loeser, C-H. Park, A.Y. Matsuura, J.N. Eckstein, I. Bozovic, P. Fournier, A. Kapitulnik, W.E. Spicer, Z.-X. Shen: Phys. Rev. Lett. **76** (1996) 4841.
- 26) T. Yoshida, X.J. Zhou, T. Sasagawa, W.L. Yang, P.V. Bogdanov, A. Lanzara, Z. Hussain, T. Mizokawa, A. Fujimori, H. Eisaki, Z.-X. Shen, T. Kakeshita, and S. Uchida: Phys. Rev. Lett. **91** (2003) 027001.
- 27) P.V. Bogdanov, A. Lanzara, S.A. Keller, X.J. Zhou, E.D. Lu, W.J. Zheng, G. Gu, J.-I. Shimoyama, K. Kishio, H. Ikeda, R. Yoshizaki, Z. Hussain, and Z.X. Shen: Phys. Rev. Lett. **85** (2000) 2581.
- 28) A. Lanzara, P.V. Bogdanov, X.J. Zhou, S.A. Keller, D.L. Feng, E.D. Lu, T. Yoshida, H. Eisaki, A. Fujimori, K. Kishio, J.-I. Shimoyama, T. Noda, S. Uchida, Z. Hussain, Z.-X. Shen: Nature **412** (2001) 510.
- 29) Y. Kakehashi and P. Fulde: Phys. Rev. B **70** (2004) 195102.
- 30) H. Mori: Prog. Theor. Phys. **33** (1965) 423.
- 31) R. Zwanzig: *Lectures in Theoretical Physics* (Interscience, New York, 1961), Vol.3.
- 32) H. Stoll: Phys. Rev. B **46** (1992) 6700; Chem. Phys. Lett. **191** (1992) 548.
- 33) J. Gräfenstein, H. Stoll, and P. Fulde, Chem. Phys. Lett. **215** (1993) 611.

- 34) J. Gräfenstein, H. Stoll, and P. Fulde: Phys. Rev. B **55** (1997) 13588.
- 35) M.H. Hettler, A.N. Tahvildar-Zadeh, M. Jarrell, T. Pruschke, and H.R. Krishnamurthy: Phys. Rev. B **58** (1998) R7475.
- 36) M. Jarrell, Th. Maier, C. Huscroft, and S. Moukouri: Phys. Rev. B **64** (2001) 195130.
- 37) G. Kotliar, S.Y. Savrasov, G. Pálsson, and G. Biroli: Phys. Rev. Lett. **87** (2001) 186401; G. Biroli, O. Parcollet, and G. Kotliar: cond-mat/0307587 (2003).
- 38) P. Sun and G. Kotliar: Phys. Rev. B **66** (2002) 085120.
- 39) Y. Kakehashi and P. Fulde: Phys. Rev. Lett. **94** (2005) 156401.
- 40) Y. Kakehashi and P. Fulde: J. Phys. Soc. Jpn. **74** (2005) 2397.
- 41) Y. Kakehashi and P. Fulde: J. Phys. Soc. Jpn. **76** (2007) 074702.
- 42) C.M. Varma, P.B. Littlewood, and S. Schmitt-Rink, E. Abrahams, and A.E. Ruckenstein: Phys. Rev. Lett. **63**, (1989) 1996.
- 43) H. Kajueter and G. Kotliar: Phys. Rev. Lett. **77** (1996) 131.
- 44) H. Schweitzer and G. Czycholl: Z. Phys. B **83** (1991) 93.
- 45) C. Gröber, R. Eder, and W. Hanke: Phys. Rev. B **62** (2000) 4336.
- 46) M.C. Gutzwiller: Phys. Rev. Lett. **10** (1963) 159.
- 47) H. Yokoyama and H. Shiba: J. Phys. Soc. Jpn, **56** 1490 (1987) 1490.
- 48) W.F. Brinkman and T.M. Rice: Phys. Rev. B **2** (1970) 4302.